ELSEVIER

Thermochimica Acta 282/283 (1996) 121–130

thermochimica acta

Kinetics and mechanism of the chalcopyrite–pyrite concentrate oxidation process[1]

Živan D. Živković [a,*], Nataša Mitevska [b], Veselin Savović [c]

[a] *Technical Faculty at Bor, 19210 Bor, Yugoslavia*
[b] *Copper Institute, 19210 Bor, Yugoslavia*
[c] *Copper Smelter and Refinery, 19210 Bor, Yugoslavia*

Abstract

The results of comparative DTA–TG–DTG analysis of the chalcopyrite–pyrite concentrate oxidative roasting process are presented in this paper. The chemistry of the process characteristic of the system investigated is defined on the basis of comparative analysis of chemical potential change in the $\log p_{SO_2}$–$\log p_{O_2}$ diagram, X-ray analysis of oxidation products at 723, 873 and 1273 K and DTA–TG–DTG results.

The activation energy values for the investigated processes are determined on the basis of DTA–TG–DTG results obtained for different heating rates by the methods of Kissinger and Ozawa.

Keywords: Activation energy; Chalcopyrite–pyrite concentrate; DTA–TG–DTG; Oxidation mechanism; Oxidative roasting; Sulphide concentrate; X-ray diffraction

1. Introduction

Physical and chemical characteristics of sulphide minerals and concentrates and their behaviour during heating (oxidative roasting) are very important for many non-ferrous metals production processes [1, 2].

Investigations of the "combustion" temperature of sulphides (beginning of desulphurization) [3, 4], and determination of the kinetics and mechanism of dissociation of some pure sulphide minerals [5, 6] are reported in the literature.

* Corresponding author.

[1] Dedicated to Takco Ozawa on the Occasion of his 65th Birthday.

PII S0040-6031(96)02883-3

Because sulphide concentrates have more complicated compositions than sulphide minerals, determination of the chemistry of processes typical of the system, demands complex investigation using comparative methods.

The mechanism of oxidative roasting of chalcopyrite–pyrite concentrate, characteristic of pyrometallurgical extraction of copper, has been determined by comparsion of results from simultaneous DTA-TG-DTG and X-ray diffraction analysis of intermediate products. Kinetic parameters for a previously defined process mechanism are also determined; these are not currently available in the literature.

2. Experimental

The concentrate from a copper mine in Bor (Yugoslavia) was used for experimental investigation of the chalcopyrite–pyrite concentrate oxidative roasting process.

The chemical composition of this concentrate was (in %): Cu–21.26; Fe–26.69; S–37.57; SiO_2–7.10; Al_2O_3–2.83; residue–4.55. The mineralogical composition of the investigated concentrate was (in %): $CuFeS_2$–53.68; FeS_2–22.19; CuS–2.19; Cu_2S–1.50; SiO_2–7.10; CaO–0.21; residue–13.13. The particle size of this concentrate was 100%–74×10^{-6} m.

For thermal investigation of the oxidative roasting process the Derivatograph 1500°C, developed by the company MOM (Budapest, Hungary) was used. The phase composition was determined on Siemens X-ray equipment with a Cu anticathode and Ni filter at a voltage of 40 kV and current of 18 mA.

3. Results and discussion

Cu–S–O and Fe–S–O systems are characteristic of chalcopyrite–pyrite concentrate. The chemical potential diagrams log p_{SO_2}–log p_{O_2} (Kellogg diagrams) for temperatures typical of the oxidation roasting process (723, 873 and 1273 K) were constructed on the basis of thermodynamic values for reactions in these systems and shown in Figs. 1 and 2.

The results obtained show equilibrium between phases:

$$Cu–Cu_2S–CuS–Cu_2O–CuO–CuO\cdot CuSO_4–CuSO_4$$

and

$$Fe–FeS_2–FeS–FeSO_4–Fe_2(SO_4)_3–FeO–Fe_3O_4–Fe_2O_3.$$

The SO_2 and O_2 concentrations in gaseous phase are from 1–10% and 1–21%, respectively.

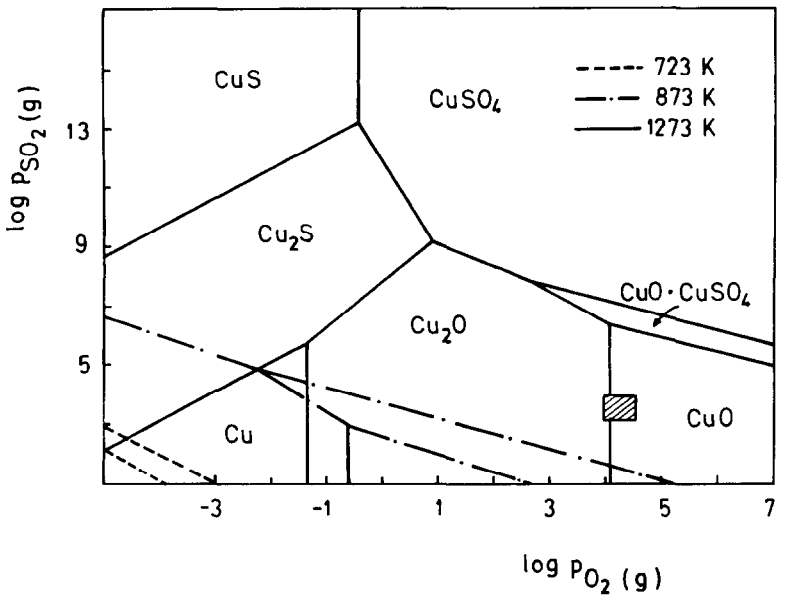

Fig. 1. Chemical potential diagram $\log p_{SO_2} = f(\log p_{O_2})$ for the Cu–S–O system at different temperatures (marked surface represents conditions during fluidized bed roasting).

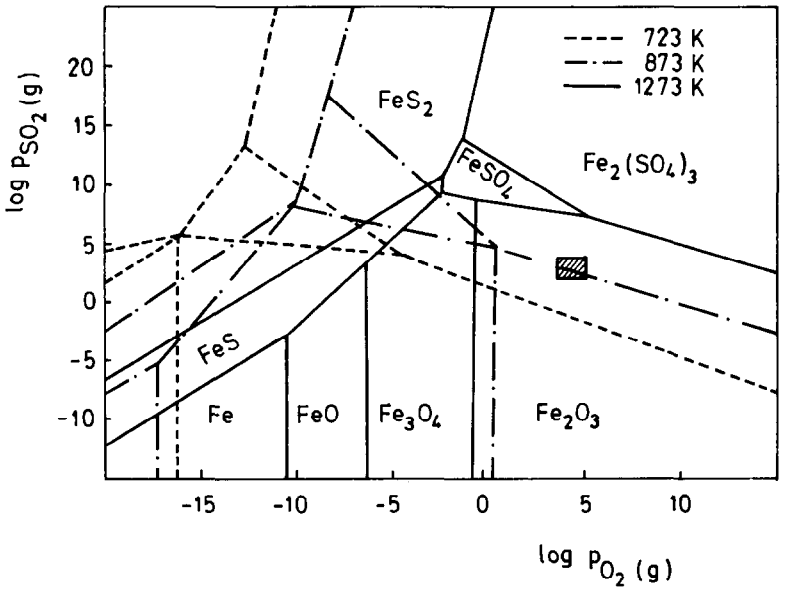

Fig. 2. Chemical potential diagram $\log p_{SO_2} = f(\log p_{O_2})$ for the Fe–S–O system at different temperatures (marked surface represents conditions during fluidized bed roasting).

The stable phases formed during oxidative roasting under industrial conditions are depending on temperature:

723 K:

$$FeS_2 \begin{cases} \rightarrow FeSO_4 \rightarrow Fe_2(SO_4)_3 \\ \rightarrow FeS \rightarrow FeSO_4 \rightarrow Fe_2O_3 \\ \rightarrow FeS \rightarrow Fe_3O_4 \rightarrow Fe_2O_3 \rightarrow FeSO_4 \rightarrow Fe_2(SO_4)_3 \end{cases}$$

$$CuS \rightarrow Cu_2S \begin{cases} \rightarrow CuSO_4 \\ \rightarrow Cu_2O \rightarrow CuO \cdot CuSO_4 \\ \rightarrow Cu_2O \rightarrow CuSO_4 \end{cases}$$

873 K:

$$FeS_2 \begin{cases} \rightarrow FeS \rightarrow Fe_3O_4 \rightarrow Fe_2O_3 \rightarrow Fe_2(SO_4)_3 \\ \rightarrow FeS \rightarrow FeSO_4 \rightarrow Fe_2(SO_4)_3 \\ \rightarrow FeSO_4 \rightarrow Fe_2(SO_4)_3 \\ \rightarrow FeS \rightarrow FeSO_4 \rightarrow Fe_2O_3 \end{cases}$$

$$CuS \rightarrow Cu_2S \begin{cases} \rightarrow CuSO_4 \\ \rightarrow Cu_2O \rightarrow CuSO_4 \end{cases}$$

1273 K:

$$FeS_2 \rightarrow FeS \begin{cases} \rightarrow Fe_2(SO_4)_3 \rightarrow Fe_2O_3 \\ \rightarrow Fe_3O_4 \rightarrow Fe_2O_3 \end{cases}$$

$$CuS \rightarrow Cu_2S \begin{cases} \rightarrow CuSO_4 \rightarrow Cu_2O \rightarrow CuO \\ \rightarrow Cu_2O \rightarrow CuSO_4 \rightarrow Cu_2O \rightarrow CuO \\ \rightarrow Cu_2O \rightarrow CuO \cdot CuSO_4 \rightarrow Cu_2O \rightarrow CuO \\ \rightarrow Cu_2O \rightarrow CuO \rightarrow CuO \cdot CuSO_4 \rightarrow Cu_2O \rightarrow CuO \end{cases}$$

The final products of the chalcopyrite–pyrite concentrate oxidation for defined concentrations of SO_2 and O_2 are $Fe_2O_3 + Fe_3O_4$ and $CuO + Cu_2O$.

The results of simultaneous DTA–TG–DTG analysis for the oxidative roasting of the investigated concentrate in air at a constant heating rate of 5° min^{-1} are shown in Fig. 3. The results obtained indicate the complexity of process. Because of this the process mechanism cannot be determined on the basis of the results from a single method. It is established that the oxidative roasting of chalcopyrite–pyrite concentrate, by analysis of the results shown in Figs. 1–3, can be presented as:

(1) At a temperature of 573 K the first exothermic effect on the DTA curve occurs with a loss of mass on the TG curve. This indicates the dissociation of chalcopyrite during which released elemental sulphur is oxidized to SO_2. A summary

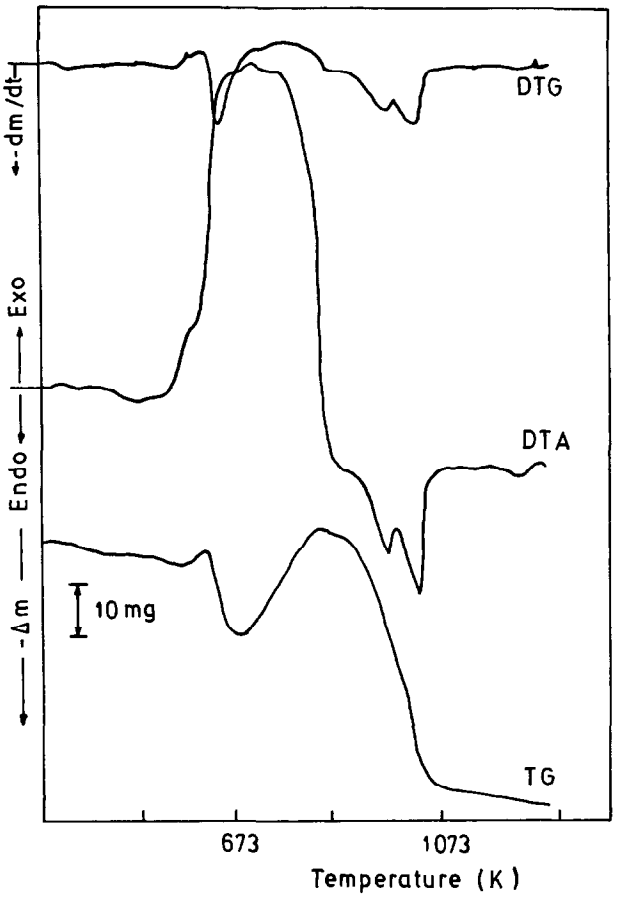

Fig. 3. DTA–TG–DTG analysis of the chalcopyrite–pyrite concentrate at a heating rate of 5° min^{-1} in air.

of this process is:

$$2CuFeS_2 + O_2 \rightarrow Cu_2S + 2FeS + SO_2 \quad (1)$$

(2) On further heating at 623 K pyrhotite, formed by dissociation of chalcopyrite, begins to be oxidized to iron sulphate, $FeSO_4$, manifested by an increase in the mass of the sample on the TG curve:

$$FeS + 2O_2 \rightarrow FeSO_4 \quad (2)$$

(3) At 643 K dissociation of pyrite [5, 7] begins, indicated by a loss of mass on the TG curve. A sharp DTG peak indicates a relatively fast process. Because this process takes place in an oxidative atmosphere, sulphur released during dissociation of pyrite is

oxidized to SO_2. Oxidation of FeS to magnetite Fe_3O_4 is also taking place. A summary of this stage of oxidative roasting is:

$$\left.\begin{aligned} &2FeS_2 \rightarrow 2FeS + S_2 \\ &S_2 + 2O_2 \rightarrow 2SO_2 \\ &3FeS + 5O_2 \rightarrow Fe_3O_4 + 3SO_2 \end{aligned}\right\} \quad (3)$$

(4) With a further increase in temperature sulphation occurs [5] causing an increase in the sample mass on the TG curve and an appropriate effect on the DTG curve. The sulphate formed becomes desulphated. A summary of this process is:

$$\left.\begin{aligned} &FeS + 2O_2 \rightarrow FeSO_4 \\ &2FeSO_4 \rightarrow Fe_2O_3 + SO_2 + SO_3 \end{aligned}\right\} \quad (4)$$

(5) The next transformation occurs at 753 K and corresponds to the oxidation of Fe_3O_4 to haematite Fe_2O_3. This process causes a further increase in the mass of the sample on the TG curve and a corresponding exothermic peak on the DTA curve:

$$4Fe_3O_4 + O_2 \rightarrow 6Fe_2O_3 \quad (5)$$

(6) At 773 K the oxidation of Cu_2S, formed by dissociation of chalcopyrite, starts, giving copper sulphates, which corresponds to further increases in mass on the TG curve. A summary of this process can be presented as:

$$\left.\begin{aligned} &Cu_2S + SO_2 + 3O_2 \rightarrow 2CuSO_4 \\ &2Cu_2S + 5O_2 \rightarrow 2(CuO \cdot CuSO_4) \end{aligned}\right\} \quad (6)$$

(7) Above 933 K complete dissociation of iron sulphate occurs:

$$2FeSO_4 \rightarrow Fe_2O_3 + SO_2 + SO_3 \quad (7)$$

(8) Finally, at temperatures above 973 K dissociation of previously formed copper sulphates occurs:

$$\left.\begin{aligned} &CuSO_4 \rightarrow CuO + SO_3 \\ &CuO \cdot CuSO_4 \rightarrow 2CuO + SO_3 \end{aligned}\right\} \quad (8)$$

The defined mechanism of chalcopyrite–pyrite concentrate oxidative roasting is confirmed by X-ray analysis of the products at 723, 873 and 1273 K, Fig. 4. Some phases formed during the oxidation (FeS, $FeSO_4$ and $CuSO_4$) are not registered on the X-ray diagrams, because there was not enough time for their crystallization.

For kinetic analysis of the process. DTA–TG–DTG curves were recorded at heating rates of 2.5, 5, 10 and 20° min^{-1}. The results obtained for the temperatures of the maxima detected on the DTA or DTG curves, depending on heating rate, are shown in Fig. 5.

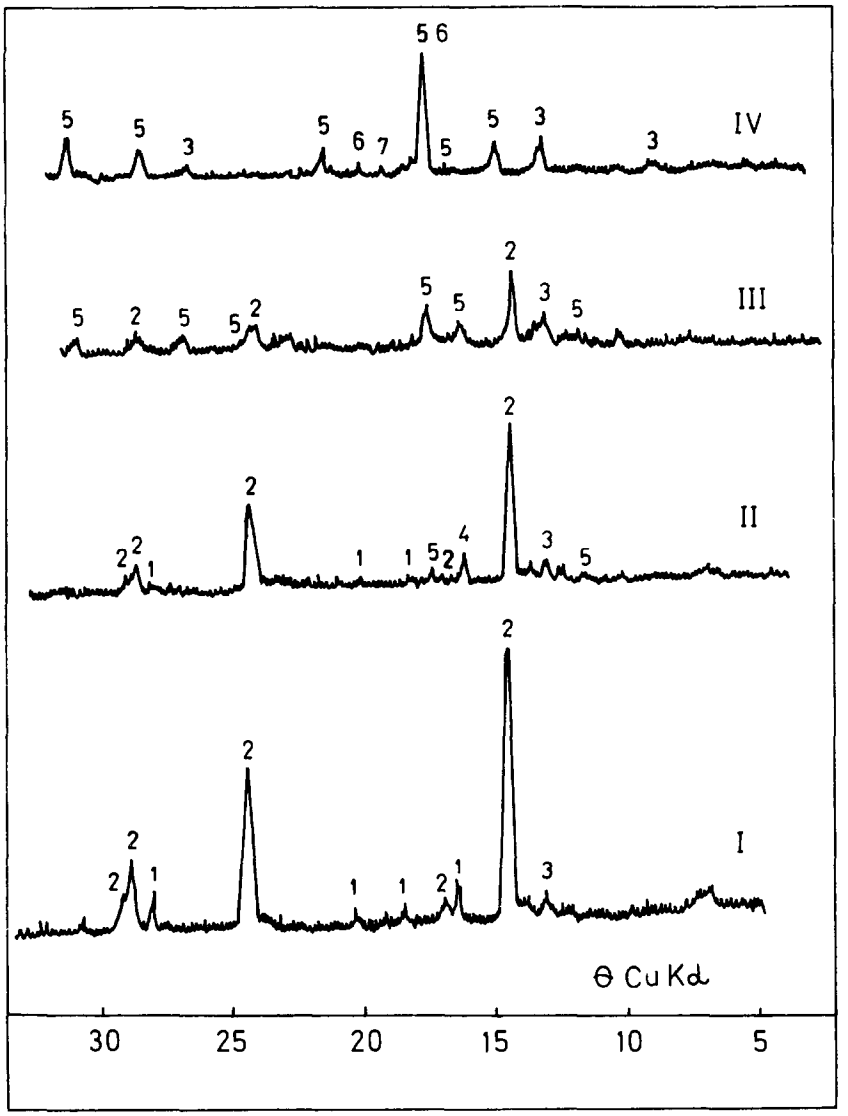

Fig. 4. X-ray analysis of chalcopyrite–pyrite concentrate (I), oxidation products at 723 K (II), 873 K (III) and 1273 K (IV); (1, FeS_2; 2, $CuFeS_2$; 3, SiO_2; 4, Fe_3O_4; 5, Fe_2O_3; 6, CuO; 7, Cu_2O).

Experimental results for the oxidative roasting of chalcopyrite–pyrite concentrate in air at different heating rates (Fig. 5) were treated according to the methods developed by Kissinger [8] and Ozawa [9] in order to determine kinetic parameters of processes (1)–(8). Fig. 6 shows the dependencies $\ln(\phi/T_m^2) = f(1/T_m)$ and $\ln \phi = f(1/T_m)$, where ϕ is the heating rate and T_m is the temperature of the maximum on the DTA or DTG curve. On the basis of these results, the corresponding values for activation energy and

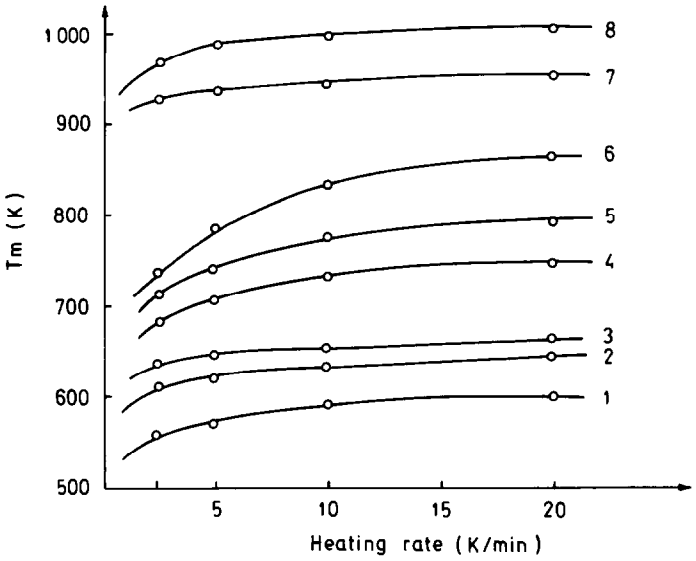

Fig. 5. Dependence of T_m on heating rate for processes (1)–(8) during the chalcopyrite–pyrite concentrate oxidation process.

the integration constants C and C_1 were calculated. The results obtained are presented in Table 1.

The results obtained indicate the complexities of the chalcopyrite–pyrite concentrate oxidative roasting process in industrial practice. Exothermic processes (1)–(6) provide enough heat energy to maintain an autogenous process in the

Table 1
Calculated values for the activation energy and integration constants for the chalcopyrite–pyrite concentrate oxidation processes

Process	Method			
	Kissinger		Ozawa	
	E/(kJ mol^{-1})	C	E/(kJ mol^{-1})	C_1
1	136	1.02×10^{8}	152	3.51×10^{14}
2	246	4.77×10^{15}	268	8.71×10^{24}
3	208	2.08×10^{11}	230	7.79×10^{18}
4	114	2.77×10^{3}	128	1.41×10^{10}
5	101	1.21×10^{2}	113	4.61×10^{8}
6	69	0.36	84	2.11×10^{6}
7	424	2.81×10^{18}	482	6.72×10^{27}
8	463	1.69×10^{24}	484	2.17×10^{34}

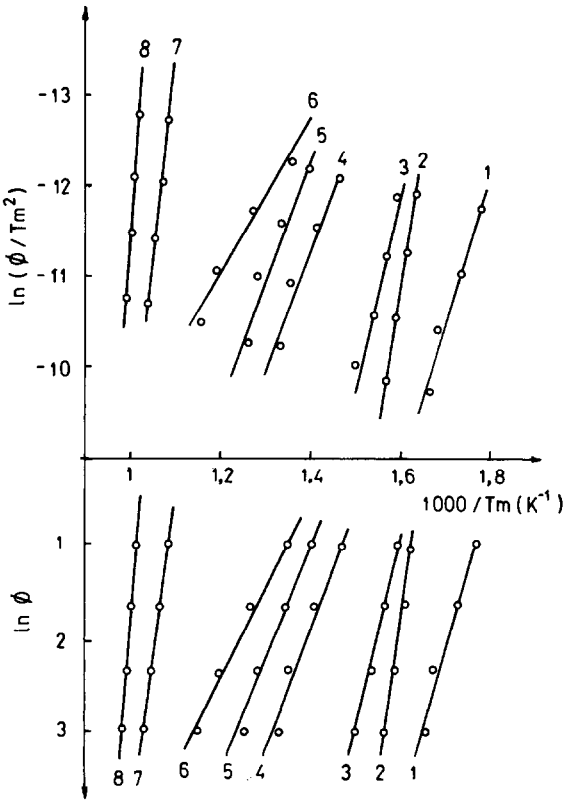

Fig. 6. Dependencies $\ln(\phi/T_m^2) = f(1/T_m)$ and $\ln \phi = f(1/T_m)$ for the chalcopyrite–pyrite concentrate oxidation process.

system after reaching the sulphide combustion temperature. Relatively high values for the activation energy indicate that most of the process is taking place on the surface of particles. An engineer can control product composition reasonably successfully by correct selection of working parameters p_{SO_2} and p_{O_2} at defined temperatures.

Under conditions of autogenous smelting of chalcopyrite pyrite concentrate the reactions (1)–(8) are very fast because the concentrate is rapidly heated to melting point. The contribution of reactions (1)–(8) to the formation of a melt of defined composition will be the subject of further research.

References

[1] A.V. Vanyukov and V. Zaitzev, Theory of the Pyrometallurgical Processes, Metallurgia, Moskow, 1973 (in Russian).

[2] Ž.D. Živković and V. Savović, Theory of the Pyrometallurgical Processes, Bor, 1994 (in Serbian).

[3] R. Dimitrov, A. Hekimova, S. Asenov, T. Ruskov and T. Tomov, Thermochim. Acta, 40, (1980) 349.
[4] R. Dimitrov and B. Boyanov, Thermochim. Acta, 64 (1983) 27.
[5] Ž.D. Živković, N. Milosavljević and J. Šestak, Thermochim. Acta, 157 (1990) 215.
[6] T. Karvan and C. Malinovski, Thermochim. Acta, 17 (1976) 195.
[7] D.J. Vaughon and J.R. Craig, Mineral Chemistry of Metal Sulphides, Cambridge University Press, Cambridge, 1978.
[8] H.E. Kissinger, Anal. Chem., 25 (1957) 1702.
[9] T. Ozawa, J. Therm. Anal., 2 (1970) 301.